

# Soliton delivery of mid-IR femtosecond pulses with ZBLAN fiber

Nikolai Tolstik,<sup>1,\*</sup> Evgeni Sorokin,<sup>2</sup> Vladimir Kalashnikov,<sup>2</sup> and Irina T. Sorokina<sup>1</sup>

<sup>1</sup>Department of Physics, The Norwegian University of Science and Technology, Trondheim, Norway

<sup>2</sup>Photonics Institute, TU Wien - Vienna University of Technology, Vienna, Austria

\*nikolai.tolstik@ntnu.no

**Abstract:** We demonstrate environmentally protected delivery of high-power femtosecond mid-IR pulses in a single-mode ZBLAN fiber by soliton formation. A 70-fs Cr:ZnS laser at 2.4  $\mu\text{m}$  reaches this regime already at  $\sim 2$  nJ launched pulse energy, while a 110-fs pulse can be transmitted without visible shortening over meters of fiber. We also measured the nonlinear-optical coefficient of ZBLAN as  $n_2 = 2.7 \pm 0.2 \times 10^{-16}$  cm<sup>2</sup>/W at 2.4  $\mu\text{m}$  wavelength.

©2012 Optical Society of America

**OCIS codes:** (060.5530) Pulse propagation and temporal solitons; (060.2390) Fiber optics, infrared; (140.3070) Infrared and far-infrared lasers.

---

## References and links

1. E. Sorokin, I. T. Sorokina, J. Mandon, G. Guelachvili, and N. Picqué, "Sensitive multiplex spectroscopy in the molecular fingerprint 2.4  $\mu\text{m}$  region with a Cr<sup>2+</sup>:ZnSe femtosecond laser," *Opt. Express* **15**(25), 16540–16545 (2007).
2. B. Bernhardt, E. Sorokin, P. Jacquet, R. Thon, T. Becker, I. Sorokina, N. Picqué, and T. Hänsch, "Mid-infrared dual-comb spectroscopy with 2.4  $\mu\text{m}$  Cr<sup>2+</sup>:ZnSe femtosecond lasers," *Appl. Phys. B* **100**(1), 3–8 (2010).
3. P. Moulton and E. Slobodchikov, "1-GW-peak-power, Cr:ZnSe laser," in *Conference on Lasers and Electro-Optics/Quantum Electronics and Laser Science and Photonic Applications Systems Technologies*, Technical Digest (CD) (Optical Society of America, 2011), paper PDPA10.
4. K. L. Vodopyanov, E. Sorokin, I. T. Sorokina, and P. G. Schunemann, "Mid-IR frequency comb source spanning 4.4–5.4  $\mu\text{m}$  based on subharmonic GaAs optical parametric oscillator," *Opt. Lett.* **36**(12), 2275–2277 (2011).
5. M. Ebrahim-Zadeh and I. T. Sorokina, *Mid-infrared Coherent Sources and Applications* (Springer, 2008), Chap. 3.
6. L. V. Doronina, I. V. Fedotov, A. A. Voronin, O. I. Ivashkina, M. A. Zots, K. V. Anokhin, E. Rostova, A. B. Fedotov, and A. M. Zheltikov, "Tailoring the soliton output of a photonic crystal fiber for enhanced two-photon excited luminescence response from fluorescent protein biomarkers and neuron activity reporters," *Opt. Lett.* **34**(21), 3373–3375 (2009).
7. D. G. Ouzounov, F. R. Ahmad, D. Müller, N. Venkataraman, M. T. Gallagher, M. G. Thomas, J. Silcox, K. W. Koch, and A. L. Gaeta, "Generation of megawatt optical solitons in hollow-core photonic band-gap fibers," *Science* **301**(5640), 1702–1704 (2003).
8. E. Garmire, T. McMahon, and M. Bass, "Flexible infrared wave-guides for high power transmission," *IEEE J. Quantum Electron.* **16**(1), 23–32 (1980).
9. V. L. Kalashnikov and E. Sorokin, "Soliton absorption spectroscopy," *Phys. Rev. A* **81**(3), 033840 (2010).
10. R. F. Bonner, L. G. Pervosti, M. B. Leon, K. Levin, and D. T. Tran, "New source for laser angioplasty: Er:YAG laser pulses transmitted through zirconium fluoride optical fiber catheters," *Proc. SPIE* **906**, 288–293 (1988).
11. E. Sorokin, N. Tolstik, and I. Sorokina, "Femtosecond operation and self-doubling of Cr:ZnS laser," in *Nonlinear Optics: Materials, Fundamentals and Applications*, OSA Technical Digest (CD) (Optical Society of America, 2011), paper NThC1.
12. E. Sorokin, N. Tolstik, and I. Sorokina, "Kerr-lens mode-locked Cr:ZnS laser," in *Lasers, Sources, and Related Photonic Devices*, OSA Technical Digest (CD) (Optical Society of America, 2012), paper AW5A.5.
13. C. Agger, C. Petersen, S. Dupont, H. Steffensen, J. K. Lyngsø, C. L. Thomsen, J. Thøgersen, S. R. Keiding, and O. Bang, "Supercontinuum generation in ZBLAN fibers - detailed comparison between measurement and simulation," *J. Opt. Soc. Am. B* **29**(4), 635–645 (2012).
14. J. M. Parker, "Fluoride glasses," *Annu. Rev. Mater. Sci.* **19**(1), 21–41 (1989).
15. E. M. Vogel, M. J. Weber, and D. M. Krol, "Nonlinear optical phenomena in glass," *Phys. Chem. Glasses* **32**, 231–254 (1991).
16. X. Yan, C. Kito, S. Miyoshi, M. Liao, T. Suzuki, and Y. Ohishi, "Raman transient response and enhanced soliton self-frequency shift in ZBLAN fiber," *J. Opt. Soc. Am. B* **29**(2), 238–243 (2012).
17. D. Klimentov, N. Tolstik, V. Dvoyrin, V. Kalashnikov, and I. Sorokina, "Broadband dispersion measurement of ZBLAN, germanate and silica fibers in MidIR," *J. Lightwave Technol.* **30**, 1943–1947 (2012).
18. G. Agrawal, *Nonlinear Fiber Optics* (Academic Press, 1989–2006).

19. E. Sorokin and I. T. Sorokina, "Ultrashort-pulsed Kerr-lens modelocked Cr:ZnSe laser," in *European Conference on Lasers and Electro-Optics (CLEO®/Europe-IQEC)*, Munich, Germany, Technical Digest (CD) (2009), paper CF1.3.
  20. V. L. Kalashnikov, E. Sorokin, and I. T. Sorokina, "Energy scaling of mid-infrared femtosecond oscillators," in *Advanced Solid-State Photonics Conference*, Technical Digest (CD) (Optical Society of America, 2007), paper WE7.
- 

## 1. Introduction

Mid-infrared femtosecond oscillators already now have numerous applications as broadband sources for sensing and molecular spectroscopy [1,2], as seed sources for amplifiers [3], and pumping sources for OPO [4]. Due to their remarkably broad spectra overlapping with water free as well as with water absorption bands of tissue they are also very promising for such medical applications as differential Optical Coherence Tomography (OCT), neurosurgery and ophthalmology [5]. They are also attractive for two-photon nonlinear microscopy, fine material processing of plastics and semiconductors, as well as for free range terrestrial and space communications. All these applications put different requirements, including e.g. broad spectral width and low noise for spectroscopic and sensing applications, high peak power for nonlinear interactions and good temporal contrast for amplifier seeding. For output of a mid-IR femtosecond oscillator to be of any use for real life applications, a way must be provided for environmentally-protected fiber beam delivery, which would not affect the spectral or temporal pulse profile. For high-energy pulses, one of the ways of delivery is to realize the soliton propagation regime [6,7].

Historically, for long pulses and continuous-wave radiation delivery the air-filled hollow core waveguides (HCW) [8] and fibers (HCF) have been used in mid-IR wavelength range. However, the broadband mid-IR femtosecond pulses are affected by both, dispersion of the air as well as by molecular absorption of the atmosphere [4,9], making it necessary, for example, to evacuate or purge the oscillators [1]. Moreover, the bending loss of HCFs constitutes an important issue for applications requiring little variation of the output power during fiber flexure. The most well developed solid-core fibers in mid-IR are fluoride, Ag halide and chalcogenide fibers, the latter having been shown to be toxic and as such, not applicable for medical use. Bonner et al [10] were the first to demonstrate the applicability of fluoride fiber for the 2.8  $\mu\text{m}$  Er:YAG laser radiation delivery for medical applications – human aorta surgery. Such fiber delivery is however, equally important for femtosecond pulse delivery into the body, least invasively through an endoscope, for making fine surgery on the brain and eye tissue as well as in-vivo imaging with high resolution (e.g. for early identification of cancerous cells).

In this work we demonstrate the first fiber delivery of the high energy femtosecond mid-IR laser pulses (70 fs), produced by the recently developed in our group femtosecond mid-IR Cr:ZnS laser [11,12]. By changing the launched pulse energy we are able to observe a transition from strongly chirped linear to solitonic propagation at launched energies below 2 nJ. The experiments and simulation indicate quite a broad range of pulse energies and fiber length where this regime can be maintained allowing practical in-house applications.

## 2. Experimental setup

The experimental setup is schematically shown in Fig. 1. As a source of the femtosecond pulses in mid-IR spectral region we used the Kerr-lens mode-locked Cr:ZnS oscillator. The laser was built on the basis of X-folded four-mirror cavity. It was pumped by the diode-pumped 5-W 1.61  $\mu\text{m}$  Er-fiber laser from IPG Photonics. The mode-locking was achieved by soft-aperture Kerr-Lens effect. The compensation of the group-delay dispersion was performed by YAG plate inserted into the cavity and chirped HR mirror. The laser produced pulses of about 68 fs with pulse repetition rate of 104 MHz at the central wavelength of 2.39  $\mu\text{m}$  and average output power up to 550 mW. The spectral bandwidth of output emission reached 88 nm, which corresponded to the time-bandwidth product of 0.315. We assume the input pulse to be essentially chirp-free.

About 85% of the laser output was delivered to the input end of the nonlinear fiber, while the other 15% of the emission were directed to the FTIR spectrometer for simultaneous control of the laser emission spectrum. The pulse durations were measured by self-developed two-photon absorption based autocorrelator. The oscillator emission was focused to the fiber input by the aspheric lens with the focal length of 8 mm. The lens was antireflection coated at the wavelength of 1.6  $\mu\text{m}$  resulting in additional losses at the laser wavelength. The fiber input facet was cut at the angle of  $82^\circ$  to exclude backreflection to the oscillator. The emission from the fiber output was collimated by AR-coated IR aspheric lens and delivered to either spectrometer or autocorrelator. The launched energy was varied by the iris installed in front of the focusing optics. The coupling efficiency reached 43%. The output pulse energy was measured after the collimating lens and assumed equal to the launched energy, as the fiber attenuation was reported to be 0.08 dB/m at 2.5  $\mu\text{m}$  [13] and the fiber is quoted single-mode in this wavelength range.

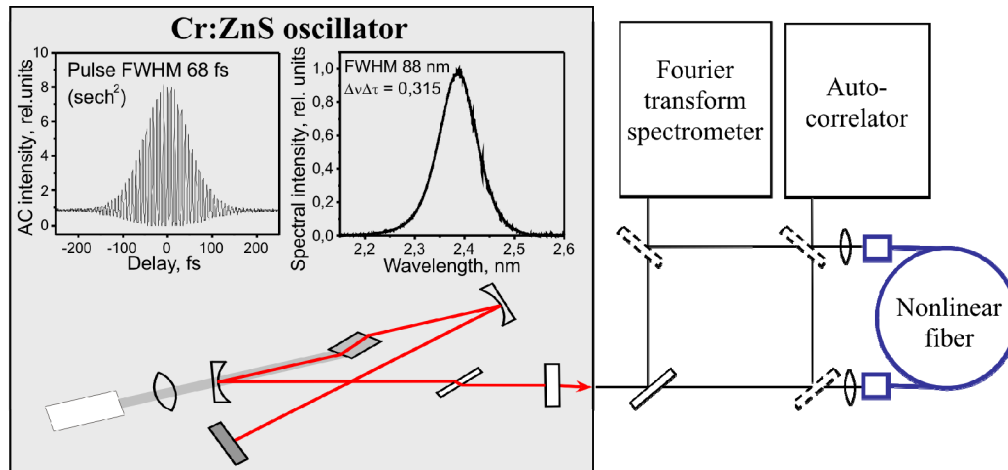


Fig. 1. Schematic setup for characterization of mid-IR femtosecond pulse propagation in nonlinear fibers.

As a nonlinear fiber we used commercially-available single-mode step-index ZBLAN fiber for infrared applications from IR Photonics. The following fiber parameters were given by the manufacturer: numerical aperture of 0.17, core diameter of 9  $\mu\text{m}$  and total length of 208 cm. These corresponded to mode area of  $A_{\text{eff}} = 96\mu\text{m}^2$ , group-velocity dispersion coefficient  $\beta_2 = -250 \text{ fs}^2/\text{cm}$  at the laser wavelength (dispersion parameter  $D \approx 8 \text{ ps}/\text{nm}\cdot\text{km}$ ), and a third-order dispersion coefficient  $\text{TOD} = 1650 \text{ fs}^3/\text{cm}$  with zero-dispersion wavelength at 1.74  $\mu\text{m}$ . An estimation using the available nonlinearity values for ZBLAN of  $n_2 = 2.1 \times 10^{-16} \text{ cm}^2/\text{W}$  [13],  $2.37 \times 10^{-16} \text{ cm}^2/\text{W}$  [14],  $3.3 \times 10^{-16} \text{ cm}^2/\text{W}$  [15] and  $5.4 \times 10^{-16} \text{ cm}^2/\text{W}$  [16] gives the pulse energy range for the  $N = 1$  soliton from 0.9 nJ to 2.3 nJ at pulse duration  $\sim 70$  fs.

### 3. Experimental results and modeling

We have performed experiments with two different pulse durations: 68 and 110 fs. The output spectra of the 68-fs pulse at  $\lambda = 2.39 \mu\text{m}$  are shown in Fig. 2(a) starting with the input pulse spectrum. Figure 3 shows these spectra (second row) with corresponding autocorrelation signals (fourth row) at characteristic energies. The data and simulations are summarized in Fig. 4(a). At low pulse energies  $\leq 0.5$  nJ the propagation is essentially dispersive (large chirp, spectrum corresponds to that of the input). At moderate pulse energies 0.5 – 1.5 nJ nonlinear effects cause the spectrum and pulse narrowing, accompanied by rapid chirp elimination. The spectrum reaches its lowest width at about 1.25 nJ, corresponding to an  $N = 0.5$  pulse in the simulated spectra evolution on Fig. 2(b). Above 1.5 nJ the spectrum gets again broadened and the chirp-free pulse approaches initial duration and spectral width, corresponding to  $N = 1$

soliton propagation. We also observe modulation of the spectral wings, as well as certain asymmetry and slight shift towards longer wavelengths at higher energy levels. The output pulse duration reached 100 fs at the highest launched energy of 2 nJ, which is lower than initial 68 fs, thus indicating that we did not yet reach the true  $N = 1$  soliton propagation. This required reassessment of the fiber parameters.

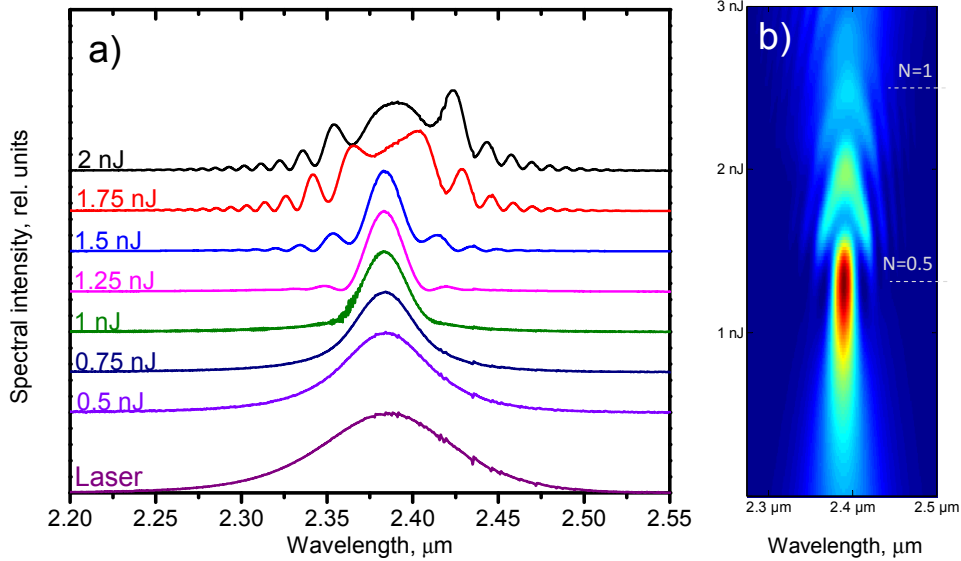


Fig. 2. Experimental spectra of a 68-fs input pulse after propagation in 2.08 m ZBLAN fiber (a) and simulated spectra (b) for the same fiber length,  $D = 11$  ps/nm-km, and  $\gamma = 0.65$  W<sup>-1</sup>km<sup>-1</sup>.

In order to recover the fiber parameters and extrapolate the results to higher energies and longer fibers we performed modeling of the pulse propagation. The propagation model was based on the generalized nonlinear Schrödinger equation solved on the basis of symmetrized split-step Fourier method with 1 fs temporal step ( $2^{17}$  points in a mesh) and a propagation step of  $10^{-3}$  part of a nonlinear length  $L_{NL}$  depending on the pulse energy. As fitting parameters we used the fiber self-phase modulation (SPM) parameter  $\gamma = 2\pi n_2/\lambda A_{eff}$  and the dispersion parameter  $D$ . The simulation results are shown along the experimental data in Fig. 2(b) (spectral evolution), Fig. 3 (spectra and autocorrelation traces) and Fig. 4(a) (pulse duration). The fiber parameters as supplied by the manufacturer resulted in very poor simulation as evidenced by the square markers in Fig. 4(a). The really good match with the experiment could be obtained only assuming the group velocity dispersion parameter of  $\beta_2 = -340 \pm 5$  fs<sup>2</sup>/cm ( $D = 11$  ps/nm-km), TOD =  $2100 \pm 200$  fs<sup>3</sup>/cm and SPM parameter  $\gamma = 0.65 \pm 0.03$  W<sup>-1</sup>km<sup>-1</sup>. Note the small error margins on dispersion and SPM parameters. This is possible because of the very high sensitivity of the position and form of the wing lobes in the autocorrelation traces to both, dispersion and SPM. The accuracy of the simulation is perfect up to the energy  $\sim 1.5$  nJ (Fig. 3), after which the measured spectrum demonstrates more asymmetry and stronger red-shift than the calculation. We attribute this to the action of the Raman self-frequency shift [13], which was not included in our model.

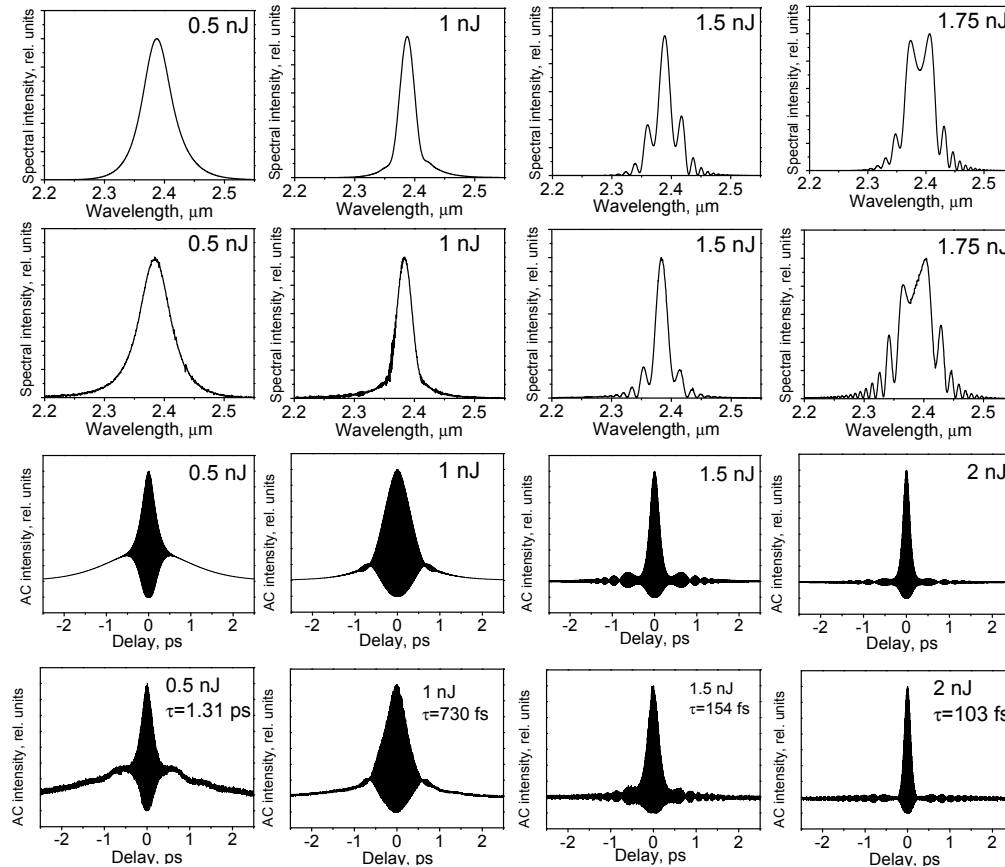


Fig. 3. Simulated (first row) and measured (second row) spectra, as well as simulated (third row) and measured (fourth row) autocorrelation traces of a 68-fs input pulse after propagation in 2.08 m ZBLAN fiber. Fiber parameters used for simulation are  $D = 11$  ps/nm-km, and  $\gamma = 0.65$  W<sup>-1</sup>km<sup>-1</sup>.

An independent confirmation of the modelling relevance comes from the direct dispersion measurements, recently performed by our group [17]. The results of the dispersion parameter measurements, as well as the modelling for two core diameter values, are shown in the Fig. 4(b) giving the value of  $D = 11.5 \pm 1.5$  ps/nm-km at 2.4  $\mu$ m, clearly higher than the 8 ps/nm-km value incurred from the nominal fiber core diameter of 9  $\mu$ m. However, if we assume the core radius of 10.5  $\mu$ m, then both the dispersion and TOD perfectly match the fitted parameters. It is very unlikely that the manufacturer could miss the nominal core diameter by such large margin. We suppose therefore that the fiber has become partially graded-index during the pulling process. This would explain larger mode diameter and the corresponding dispersion shift. Assuming the new diameter and the fitted SPM parameter we can estimate the effective mode area  $A_{\text{eff}} = 110 \pm 5$   $\mu$ m<sup>2</sup> giving the nonlinear coefficient  $n_2 = 2.7 \pm 0.2 \times 10^{-16}$  cm<sup>2</sup>/W. This value is close yet higher than the  $2.37 \times 10^{-16}$  cm<sup>2</sup>/W value of [14] and lower than the  $3.3 \times 10^{-16}$  cm<sup>2</sup>/W value of [15]. The  $5.4 \times 10^{-16}$  cm<sup>2</sup>/W from [16] could not be confirmed. An independent estimation of the effective area from the mode profile measurements gives even higher value of  $A_{\text{eff}} = 135 \pm 30$   $\mu$ m<sup>2</sup>, but with a much bigger uncertainty than the value obtained from the pulse propagation simulation.

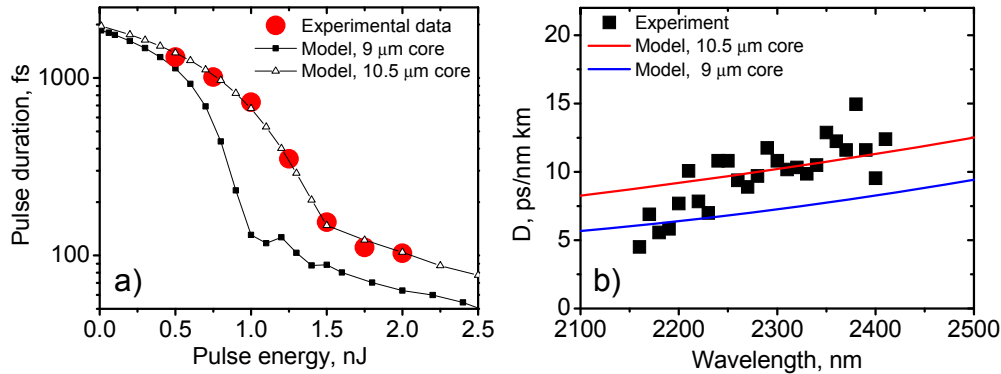


Fig. 4. Measured and simulated pulse durations at the fiber output for a 68-fs pulse (a). Measured [17] and simulated dispersion for fiber with different core diameters (b).

The corrected parameters allows predicting that the true  $N = 1$  soliton at maximum 2 nJ energy can be reached for pulse durations  $\tau \geq 100$  fs. The laser source has been adjusted to provide 110-fs pulses at the same central wavelength and output energy. The exact  $N = 1$  soliton for this pulse duration has been calculated from the area theorem  $E = 3.53|\beta_2|/\gamma\tau = 1.65$  nJ. Indeed, at 1.69 nJ we observe pulse duration to return to the original value of  $\sim 110$  fs (Figs. 5(a) and 5(b)). At the same time the spectrum of the pulse acquires red-shift and retains some uncompensated modulation (Fig. 5(c)). We suggest that this is due to the influence of stimulated Raman scattering, analogously to the 68-fs pulse (Fig. 2). A simulation taking only  $n_2$  and dispersion into account produces a smooth input-like spectrum.

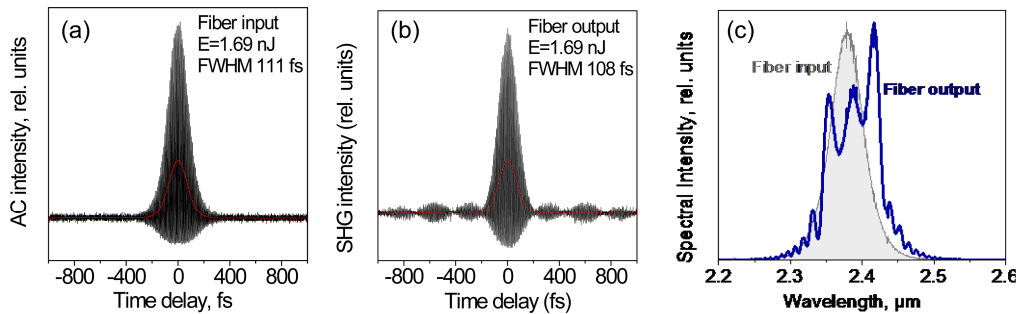


Fig. 5. Measured autocorrelation signals at fiber input (a) and output (b) for energy  $E = 1.7$  nJ, corresponding to soliton number  $N = 1.03$ . (c) Spectra at the fiber input (filled grey area) and at the output (blue curve).

The very good agreement of the simulation with the experiment allows using this model to analyze output parameters for even higher launched energies up to 5 nJ (Figs. 6(a) and 6(b)) and to follow the pulse evolution inside the fiber (Figs. 6(c) and 6(d)), extending the analysis to longer fibers. We can conclude from this simulation, that after reaching the soliton propagation regime above 1.3 nJ ( $N = 0.7$ ) the pulse remains fairly stable in the range of energies from  $\sim 1.5$  to  $\leq 5$  nJ ( $N = 3$ ), when the pulse starts to shed the energy. Due to the finite fiber length this range is somewhat different from the theoretical soliton stability range of  $0.5 < N < 1.5$  [18]. The pulse parameters remain fairly constant along the propagation distance (Figs. 6(c) and 6(d)). Summarizing, this simulation shows that there exist quite broad range of energies and lengths, where pulse can propagate retaining its duration and without critical, meaning that ZBLAN can be used in practice for mid-IR femtosecond pulse delivery for typical in-house distances of few meters.

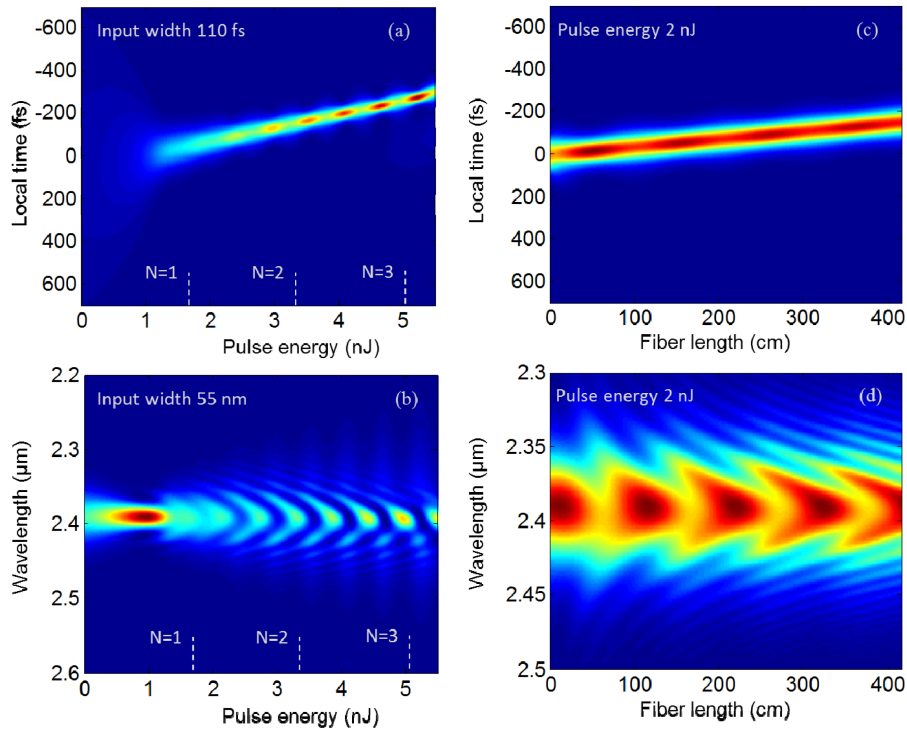


Fig. 6. Simulated intensity (a) and spectrum (b) at the output of a 208-cm long fiber for a 110-fs input pulse and varying pulse energy. Simulated intensity (c) and spectrum (d) evolution inside the fiber for a 2-nJ 110-fs pulse calculated for fiber lengths up to 416 cm. The drift with respect to the local time frame and spectral asymmetry are due to the third-order dispersion.

#### 4. Conclusion

We have successfully tested a single-mode ZBLAN fiber for mid-IR femtosecond pulse delivery. At low launched energies  $< 1$  nJ the propagation is essentially linear with negligible spectrum modification. This regime is suitable for spectroscopic and sensing applications, providing means of environmentally protected signal delivery between sealed units.

At higher powers, the solitonic effect starts to dominate, resulting in rapid pulse shortening. This regime is suitable for high-power pulse delivery. For example, at 2 nJ and 110 fs pulse duration, the peak power reaches 18 kW, which is over 10 times higher than the threshold for subharmonic OPO pumping at this wavelength [4]. The regime is not critical to pulse energy and fiber length variations in quite broad range, making it practical for in-house applications.

Pulse energies of few nJ at 50-100 fs pulse duration are quite feasible for Cr:ZnS and Cr:ZnSe [19] oscillators, and fulfill conditions for solitonic propagation in commercially available single-mode ZBLAN fibers. For delivery of significantly higher energies, one should consider transition to LMA fibers. Increase of an effective mode area to  $\sim 1500 \mu\text{m}^2$  allows the energy scaling up to  $\sim 30$  nJ that is feasible for the chirped pulse oscillators [19,20]. Since the pulse is pre-chirped in this regime, its squeezing in anomalously dispersive fiber would allow achieving sub-MW power levels on a target.

The nonlinear-optical coefficient of ZBLAN has been measured to be  $n_2 = 2.7 \pm 0.2 \times 10^{-16} \text{ cm}^2/\text{W}$  at 2.39  $\mu\text{m}$  wavelength.

## **Acknowledgments**

This work was supported by the Norwegian Research Council (NFR) projects FRITEK/191614 and MARTEC-MLR as well as the Austrian Science Fund (FWF project P17973). We also acknowledge IR Photonics for providing the ZBLAN fiber.